Article

An Experimental Investigation of the Effect of Two-Phase Flow in a Manifold on Water Jet Lengths

Seyhmus Tumur * , **Arjin Ata and Tamer Bagatur**

Department of Civil Engineering, Dicle University, Diyarbakir 21280, Turkey; arjinata@gmail.com (A.A.); tbagatur@dicle.edu.tr (T.B.)
* Correspondence: stumur@dicle.edu.tr

Abstract: The outlet flow rates and changes in behaviors of five outlet ports where water and air–water (two-phase) mixtures pass horizontally in a manifold pipe system were investigated experimentally. The effects of different air-flow rates, vacuumed from the atmosphere with a Venturi device in the system, on the outlet flow rates and diameters of the manifold port outlets were compared by measuring the outlet jet lengths. The system performance provided homogeneity of manifold port outlet flows and was tested. As a result, it was observed that homogeneous jet lengths were obtained in both single and two-phase low main manifold flows and equal outlet port diameters. When the main manifold flow rate V is 1.5–2 m/s, the system is stable and produces high jet lengths. The manifold pipe systems used in the experimental setup provide suitable working conditions for d/D = 0.433. The system does not show a smooth flow pattern with Venturi devices for d/D < 0.433. The low flow rates in this study's tests are key. They are vital for designing micro irrigation systems. This depends on the critical d/D ratio of the system.

Keywords: manifold; water jet; two-phase flow

1. Introduction

In water resource engineering, fluid flows have two models. They are pressurized and free surface flow models. These applications can be seen in irrigation systems, treatment plants, and hydraulic structures [1]. Fluid flows can exhibit single-phase or two-phase flow characteristics. In particular, air–water mixtures are used to transfer oxygen from the atmosphere in aeration systems. Aeration is generally carried out for oxygen transfer to water, mixing, and flotation [2]. Besides traditional aerators like mechanical aerators and pressurized diffusers, water jet aeration systems are also used. Water jets play a significant role in air transmission, dispersing transmitted air as air bubbles within the water mass and effectively contacting the air–water mixture. In practical applications, jet aerators are used in the field of chemical engineering for mixing processes and enhancing gas–liquid transfer. In environmental engineering, they are preferred for mixing and oxygen transfer processes in drinking water and wastewater treatment plants [3]. Moreover, Venturi-type aerators have become widely used in recent times. In these flow systems, the air absorbed depending on various parameters enters the system as small bubbles [4].

Integrating different scale designs of system elements of this study into experimental setups may be the subject of subsequent studies. It is also thought that the dimensionless equations obtained in the article will contribute to the analysis of experimental accuracy.

This thesis aims to experimentally investigate the variations in exit flow values and behaviors of water and air–water mixture flow models passing through a horizontally placed manifold pipe system according to different port exit diameters.

In this study, Venturi aerators for air transfer and a manifold with different port exit diameters were used. In these systems, a transition from high-pressure two-phase flow to low-pressure flow occurs [5].

The experimental infrastructure of the study aims to investigate the variations in exit flow values and behaviors of water and air–water (two-phase) mixture flow models passing through a horizontally placed manifold pipe system according to different port exit diameters. In this context, the effect of different air–water flow rates on the manifold port exit diameters and exit flows will be compared with measurements of exit jet lengths. The most fundamental results aimed to be achieved will be to investigate the most ideal system performance ensuring homogeneous manifold port exit flows.

Additionally, it is planned to investigate the air transfer efficiency corresponding to varying water flow rates using two different types of Venturi devices in this study.

Homogeneous water distribution in irrigation systems plays a critical role in the optimal use of irrigation water, directly affecting water use efficiency and crop production. To evaluate the effects of wind on sprinkler water distribution, it is important to measure on-site water distribution under different wind conditions and then calculate the parameters that describe water distribution. The study by Carrión, Tarjuelo, and Montero (2001) [6] enhances the SIRIAS simulation model for sprinkler systems, which can be used for the design of new irrigation systems or the improvement of existing ones. The model, which simulates the trajectories of droplets sprayed by sprinklers using ballistic theory, employs a new air resistance coefficient formulation to calculate wind-disturbed water distribution. Additionally, it offers three options to account for evaporation and drift losses during the irrigation process. The SIRIAS software (version 2000) was developed for Windows 95, 98, and NT using the Delphi programming language.

In the study conducted by Issaka et al. (2018) [7], significant challenges encountered in addressing the impact of climate change on agricultural production through sprinkler irrigation were discussed. It was emphasized that optimizing the performance of fixed water distribution devices in smart sprinkler irrigation systems under low pressure justifies the investment cost and achieves the desired droplet sizes that minimize evaporation losses and wind-induced distribution distortions while maintaining large throw distances.

The study by Kaur et al. (2020) concluded that the adoption of micro-sprinkler irrigation, compared to traditional irrigation methods, results in increased water use efficiency (60–80%), water savings (20–60%), reduced fertilizer requirements (20–33%), higher quality crop production, and increased yield (7–25%) [8].

The study by Subaschandar and Sakthivel (2016) [9] used computational fluid dynamics (CFD) methodology to analyze the flow characteristics within a manifold. It was found that the original geometry exhibited flow non-uniformity in terms of mass flow rates and outlet temperatures. The minimal mixing of hot and cold-water flows within the manifold led to erroneous distributions in mass flow rates and temperatures at the outlets. Based on preliminary results, a design modification was implemented by adding two humps to the vertical pipe along the flow direction. The results showed a significant reduction in the erroneous distribution of mass flow rates and temperatures at the outlets. This simple design modification was shown to improve flow quality by providing nearly equal mass flow rates and temperatures at the outlets. The study demonstrated that the CFD methodology could be effectively and successfully used to analyze and improve flow quality within a manifold.

The study by Hassan et al. (2014) [10] aimed to evaluate the hydraulic parameters of the manifold to achieve uniform mass flow at the manifold outlet. In this study, CFD simulation and experimental data were conducted with different outlet configurations, namely, circular and conical sections. While severe maldistribution was obtained at the outlet of the circular-sectioned manifold, uniform flow was achieved in the conical-sectioned manifold. A numerical model was used to predict the flow along each lateral for three different Reynolds numbers (100,000, 150,000, and 200,000), and it was found that the results exhibited the same trend when compared with experimental data. The study concluded that flow distribution in manifolds is independent of the Reynolds number, as the Reynolds number had a minimal effect on the uniformity of mass effusion from the outlets.

The study by Alawee, Hassan, and Mohammad (2021) [11] examined the methodology of flow uniformity at the distribution manifold inlet, which expresses the variability in the inlet area. The baseline case for these variabilities has a diameter of 100 mm, and the range is between 100 and 50 mm. The diameter of the distribution manifold (D1) was kept constant, and the flow entered the manifold at a right angle. For all cases, the inlet water flow rate was 790 L/min. The results of this study showed that the methodology of changing the cross-sectional area from the main pipe to the manifold is a negative step in the quest for flow uniformity, as the irregularity coefficient increased from 0.3 to 0.401.

The study by Jiang et al. (2022) [12] aimed to determine the role of area ratio (AR) and Reynolds number in the distribution of flow and pressure within a partition manifold. For this purpose, five different models were used for analysis under test conditions. The first physical model consisted of a main manifold with a diameter of 101.6 mm (4 inches) in a regular longitudinal section and five laterals with a diameter of 50.8 mm (2 inches) spaced 220 mm apart. This model was used to determine the magnitude of distributed flow that typically occurs in this type of design. The other four models used different diameters, with header diameters of 101.6, 76.2, and 50.8 mm and lateral diameters of 50.8, 38.1, and 25.4 mm. These models were used to test flow and pressure distribution based on AR. Three different values of inlet flow rates, 625, 790, and 950 L/min, were examined with the models used. The results indicated that the AR parameter has a significant effect on the uniformity of flow from the manifold; as AR decreased from 0.48 to 0.13, flow uniformity increased by 76%. It was found that within the tested Reynolds numbers (50,000–200,000), the degree of consistency in mass discharge from the laterals was not affected.

The study by Han et al. (2005) revealed that sludge accumulation on the membrane surface decreased with increasing aeration rates (0–25 L/min), but this effect did not increase linearly with the aeration rate and was neglected when the critical aeration rate was exceeded [13].

In the study conducted by Brijesh and Sagar (2016), the effects of changes in geometrical parameters (diffuser angle) on its performance were investigated. A series of experiments were conducted to study the performance of jet pump. The performance of a jet pump is defined by three sets of curves, namely, flow rate outlet, input power outlet, and efficiency outlet. Changing the diffuser angle will affect the jet pump behavior. It was found that the Venturi diffuser angle is an important geometrical parameter to characterize the maximum suction head of the jet pump [14].

Mayer, Braun, and Fuchs [15] optimized not only the aeration rate but also the diffuser nozzles delivering air to the membrane surface. The uniform aeration distribution of 10 different aeration elements, including injectors, tubes, disks, and membrane diffusers with orifice diameters ranging from 0.05 mm to 4 mm, was investigated. According to this study, micro-membrane diffusers provided uniform aeration along the tubular membrane module, but these diffusers were the most complex aeration elements examined, and their effectiveness in reducing membrane fouling was not evaluated.

In the study titled "Remote Controlled Automatic Irrigation System Design and Implementation" by Çakır et al., a remote-controlled automatic irrigation system was implemented with the PIC 16F877 microcontroller control circuit [16].

Sudharshan et al. (2019) have worked on the idea of automatic irrigation systems. They used three important sensors in the system. These sensors are soil moisture sensor, humidity sensor, and temperature sensor. They examined the data they obtained by using these sensors. They provided the power needed in the system they designed from solar panels. Thanks to the automatic smart irrigation system, they determined how often the land would be irrigated with the data they received from various sensors such as fuzzy logic, humidity, and DHT sensors. With the system they designed, they prevented a significant waste of resources and reduced the need for manpower, allowing more land to be used [17].

In the study conducted by Steven R. (2008), the researchers performed dimensional analysis with a Venturi meter placed in horizontal flow. The derived dimensional groups

were compared with Doppler meter output data, and correlations were established. As a result of the results, the obtained dimensionless numbers can be used in industrial processes. It was seen that horizontal flows are preferable in two-phase flows and should be explored in possible future studies [18].

An experimental study on the breakup of a turbulent round-water jet in still air with a nozzle Reynolds number of 145,600 and Weber number of 10,400 is reported. The visual structure of the falling water jet was recorded by a high-speed camera, and the characteristics of the falling jet were investigated. As the jet traveled from the nozzle, initial surface disturbances grew, and the lateral oscillation of the jet surface was amplified. The jet thickness initially increased and then decreased because of the combined effects of lateral turbulence fluctuation and gravitational acceleration. The amplitude of the surface disturbance grew in an exponential form. Based on the averaged transverse-water distribution, the water jet spreading rate was found to vary between 0.5 and 1.8%, and the decay of the jet water core had an average value of 0.7%. The onset of jet breakup was found at a distance of approximately 100 times the nozzle diameter. A theoretical model was developed for predicting the onset of jet breakup by comparing the dynamic air pressure with the restraining surface tension pressure. The velocity of the water drops released after breakup was measured and found to be approximately 0.8 times the local jet velocity [19].

2. Materials and Methods

2.1. Materials

The experimental setups for this study were established and tested in the Hydraulics and Environmental Laboratory of the Civil Engineering Department at Dicle University. The general view of the experimental setup is provided in Figure 1.

Figure 1. Test setup (pump, water flow meter, air-flow meter, Venturi device, and manifold).

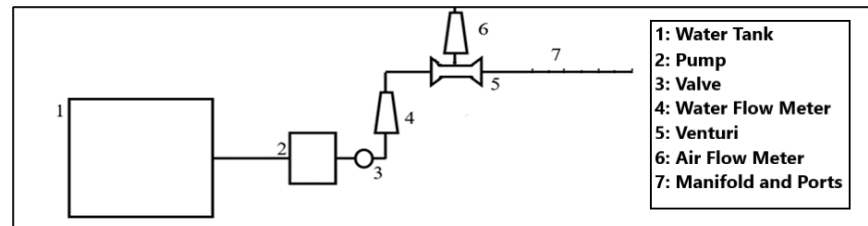The schematic views of the experimental setups are given in Figures 2 and 3.

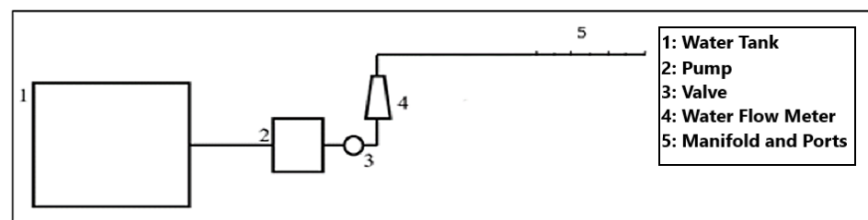**Figure 2.** Experimental setup with Venturi device.

Figure 3. Experimental setup with Venturi deviceless device.

The experimental investigation focused on the changes in the output flow values and behavior of water and air–water (two-phase) mixture flow models passing through a horizontally placed manifold pipe system. The study aimed to examine the effects of different air–water flow rates on the manifold port exit diameters and their impact on the output jet lengths. For this purpose, four different systems were designed, and water circulation was carried out at different flow rates from a 300 L water tank into a manifold pipe system with a length of 250 cm and an inner diameter of 12.7 mm, having five port exits.

In the experimental setup, a water flow meter (0–6 m^3/h., 10.1325 Pa) was used to measure the flow rate of water circulated by a water pump (0.75 kW, Pedrollo Model, Pedrollo S.p.A., Verona, Italy). The temperature inside the water tank was measured using a thermometer (WTW Tetra Con 325 Model, WTW, Troistedt, Germany). The amount of air passing through two different Venturi devices integrated into the system was measured with an air-flow meter (0.3–3.0 L/min, LZT 6-M, Changzhou City, JIangsu Prov., China). The system was leveled horizontally and vertically using a spirit level. The water jet lengths at the outlet ports for different air–water flow rates were measured with a steel tape measure according to varying port diameters.

Two different types of Venturi devices were used in this study (Figure 4). The technical specifications of these Venturi types are provided in Tables 1 and 2. The dimensions of the Venturi devices used in this study comply with ASME standards [20]. Different water flow rates, air vacuum flow rates, and transfer efficiencies were experimentally examined.
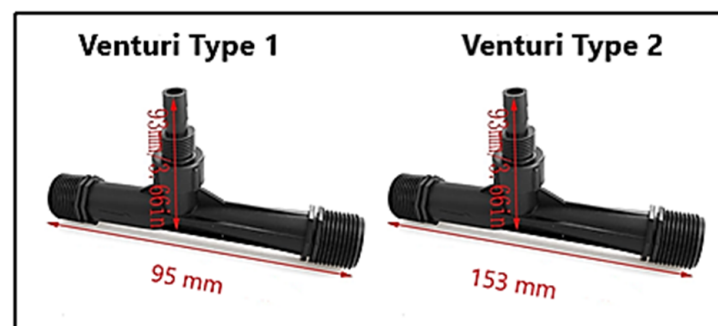

Figure 4. Types of Venturi used in the experimental set.

**Table 1.** Features of the Type 1 (Model 25100) Venturi device used in the experiment.

Water Inlet/Outlet	1.27 cm
Air Suction Nozzle	0.635 cm
Air Suction Capacity	4–7 Nm^3/h
FInlet Pressure	4.92 kg/cm^2
Water Flow Amount	400–1200 L/h
Full size	95 mm

Table 2. Features of the Type 2 (Model 25152) Venturi device used in the experiment.

Water Inlet/Outlet	1.905 cm
Air Suction Nozzle	0.635 cm
Air Suction Capacity	7.5–10 Nm^3/h
Inlet Pressure	2.04–5.098 kg/cm^2
Water Flow Amount	1000–3000 L/h
Full size	153 mm

The Venturi devices, whose specifications are given in Tables 1 and 2, were integrated into the experimental setups and operated in the laboratory at flow rates of 0.60 m^3/h., 0.75 m^3/h., 0.85 m^3/h., and 1.0 m^3/h..

Figure 5 shows the technical parameters of the manifold and ports used in the experimental setup. Four types of manifolds were designed based on different port exit diameters. Detailed information about these manifolds is provided below:
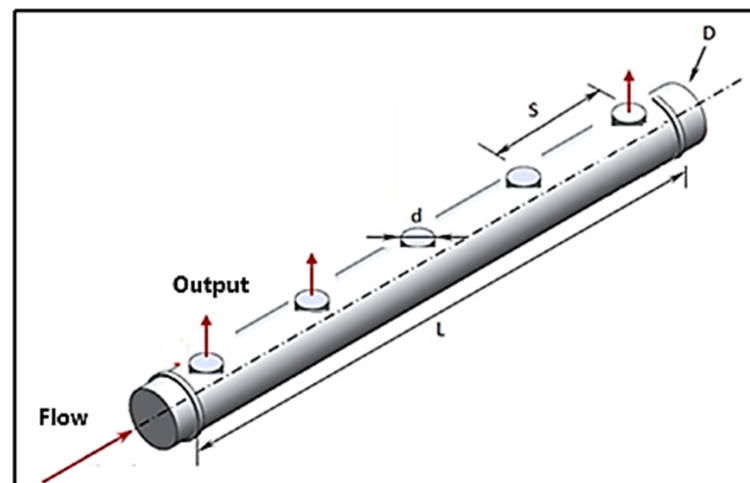
Figure 5. Manifold parameters (D = manifold main pipe diameter (1.27 cm), d = port outlet diameter (variable), L = manifold main pipe length (250 cm), and S= distance between ports (20 cm)).

(a) Manifold Type I: The system is 250 cm in length with port intervals of 20 cm. The port exit diameters are 5.5 mm, 5.5 mm, 5.5 mm, 5.5 mm, and 5.5 mm, respectively.
(b) **Manifold Type II**: The system is 250 cm in length with port intervals of 20 cm. The port exit diameters are 6.5 mm, 6.0 mm, 5.5 mm, 5.5 mm, and 5.5 mm, respectively.
(c) **Manifold Type III**: The system is 250 cm in length with port intervals of 20 cm. The port exit diameters are 7.5 mm, 7.0 mm, 6.5 mm, 6.0 mm, and 5.5 mm, respectively.
(d) **Manifold Type IV**: The system is 250 cm in length with port intervals of 20 cm. The port exit diameters are 5.5 mm, 6.0 mm, 6.5 mm, 7.0 mm, and 7.5 mm, respectively.

The changes in output flow values and behaviors of water and air–water (two-phase) mixture flow models passing through four different horizontally placed manifold pipe systems were experimentally investigated based on varying port exit diameters. The effects of different air–water flow rates on the manifold port exit diameters and their impact on the output jet lengths were compared through measurements.

2.2. Method

The method followed in this study is as follows: The experimental measurements primarily focused on determining the jet exit length based on different jet exit diameters, different main pipe flow rates, and air suction flow rates, depending on whether the system includes a Venturi or not. For the experimental measurements, the nozzle diameter was selected as $d_0 = 5.5$–7.5 mm; the main pipe flow rate as $Q_s = 17$–27.8×10^{-5} m^3/s, and $Q_a = 1.25$–4.6×10^{-5} m^3/s. Tap water was used in the measurements conducted for this study. Efforts were made to keep the working temperature stable at approximately 20 °C. Care was taken to ensure that the main flow pipe used in the experimental setup was horizontally balanced (Figure 6).

Figure 6. View of water jets issuing from the manifold and ports.

2.3. Measuring Jet Lengths

In this study, changes in the water jet exit lengths were observed depending on different nozzle exit diameters in systems with Venturi Type 1 and Venturi Type 2 and without a Venturi. Experimental studies were conducted for each different jet nozzle diameter and flow condition (Figure 6).

2.3.1. Comparison of Jet Exit Length Measurements in Open and Closed Venturi Type 1 Systems and Systems Without Venturi

In this experiment set, the aim was to compare the jet exit lengths obtained while using Venturi Type 1, Manifold Type 1, and the system without Venturi. The jet exit lengths were obtained for each nozzle with exit diameters of $d_1 = 5.5$ mm, $d_2 = 5.5$ mm, $d_3 = 5.5$ mm, $d_4 = 5.5$ mm, and $d_5 = 5.5$ mm and corresponding velocities of $V_1 = 1.34$ m/s, $V_2 = 1.64$ m/s, $V_3 = 1.86$ m/s, and $V_4 = 2.20$ m/s for both the Venturi and non-Venturi systems. The results are shown in Figure 7.

From this experiment set, it was observed that there was no change in the jet exit lengths based on constant nozzle exit diameters and flow rates. It was also observed that jet exit lengths increased with increasing flow rates for a constant nozzle exit diameter in the system. Additionally, it was noted that in the absence of a Venturi device, the jet lengths

were much larger compared to the cases where the Venturi device was closed or open. As a result, it was measured that homogeneous jet lengths were obtained at low main manifold flows and equal port exit diameters.
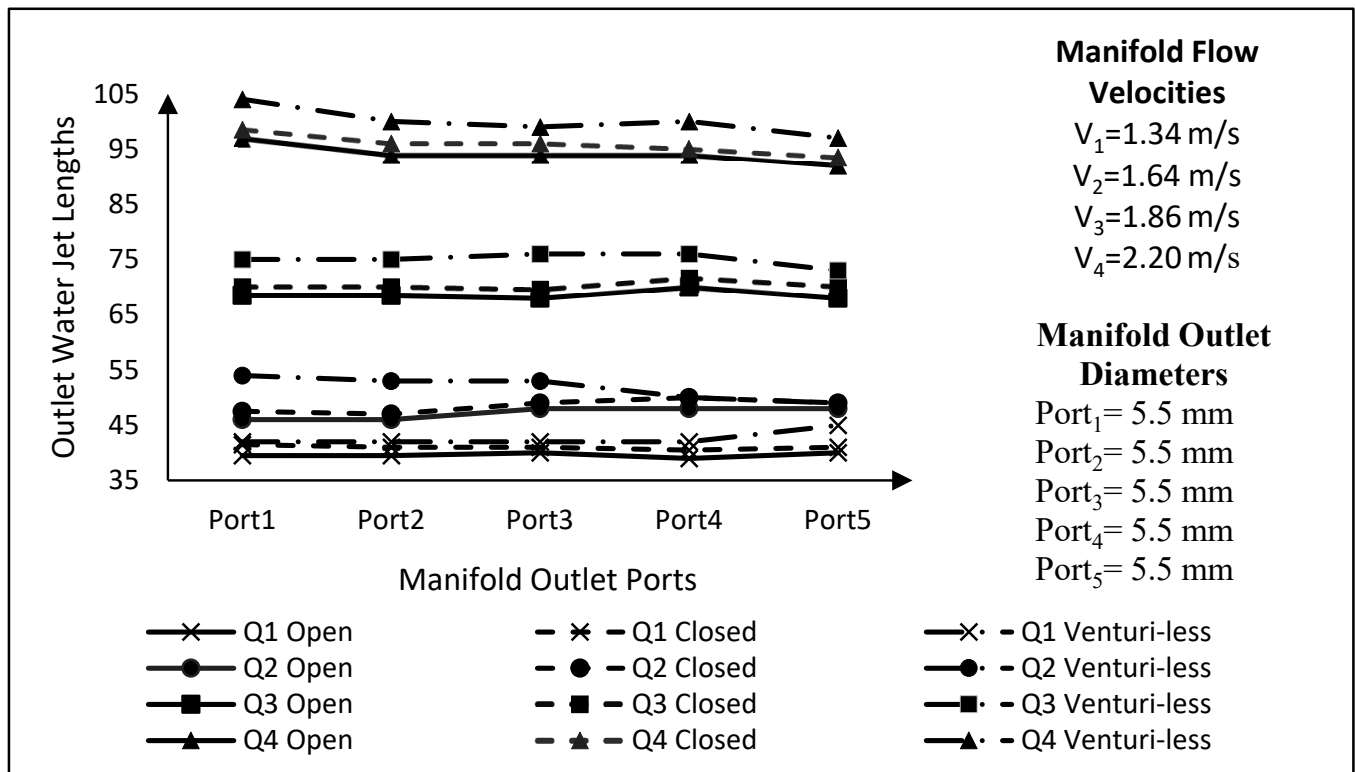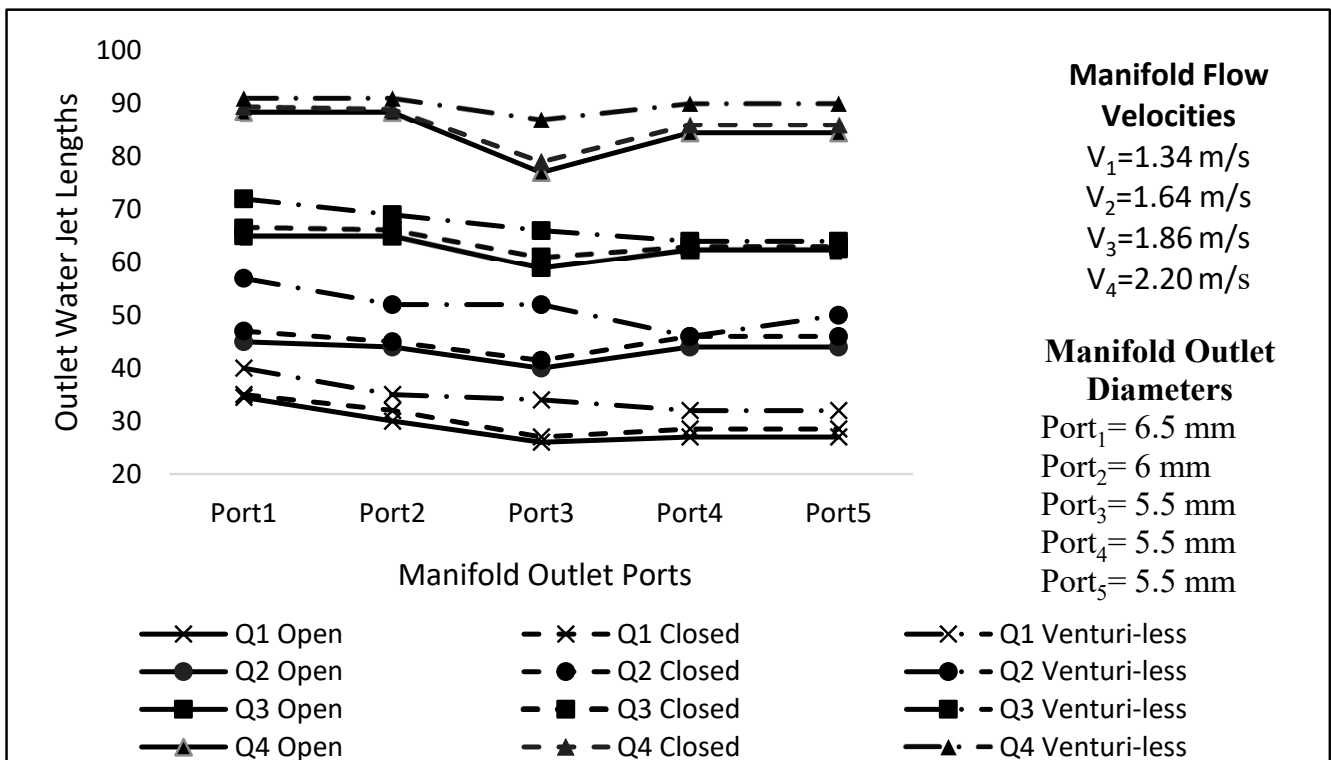

Figure 7. Graph of comparison of water jet lengths in Venturi Type 1 Manifold Type 1 open, closed, and Venturi deviceless systems ($Q_1 = 17 \times 10^{-5}$ m^3/s, $Q_2 = 20.8 \times 10^{-5}$ m^3/s, $Q_3 = 23.6 \times 10^{-5}$ m^3/s, $Q_4 = 27.8 \times 10^{-5}$ m^3/s).

In the second experiment set, the aim was to compare the jet exit lengths obtained while using Venturi Type 1, Manifold Type 2, and the system without Venturi. The jet exit lengths were obtained for each nozzle with exit diameters of $d_1 = 6.5$ mm, $d_2 = 6$ mm, $d_3 = 5.5$ mm, $d_4 = 5.5$ mm, and $d_5 = 5.5$ mm and corresponding velocities of $V_1 = 1.34$ m/s, $V_2 = 1.64$ m/s, $V_3 = 1.86$ m/s, and $V_4 = 2.20$ m/s for both the Venturi and non-Venturi systems. The results are shown in Figure 8.
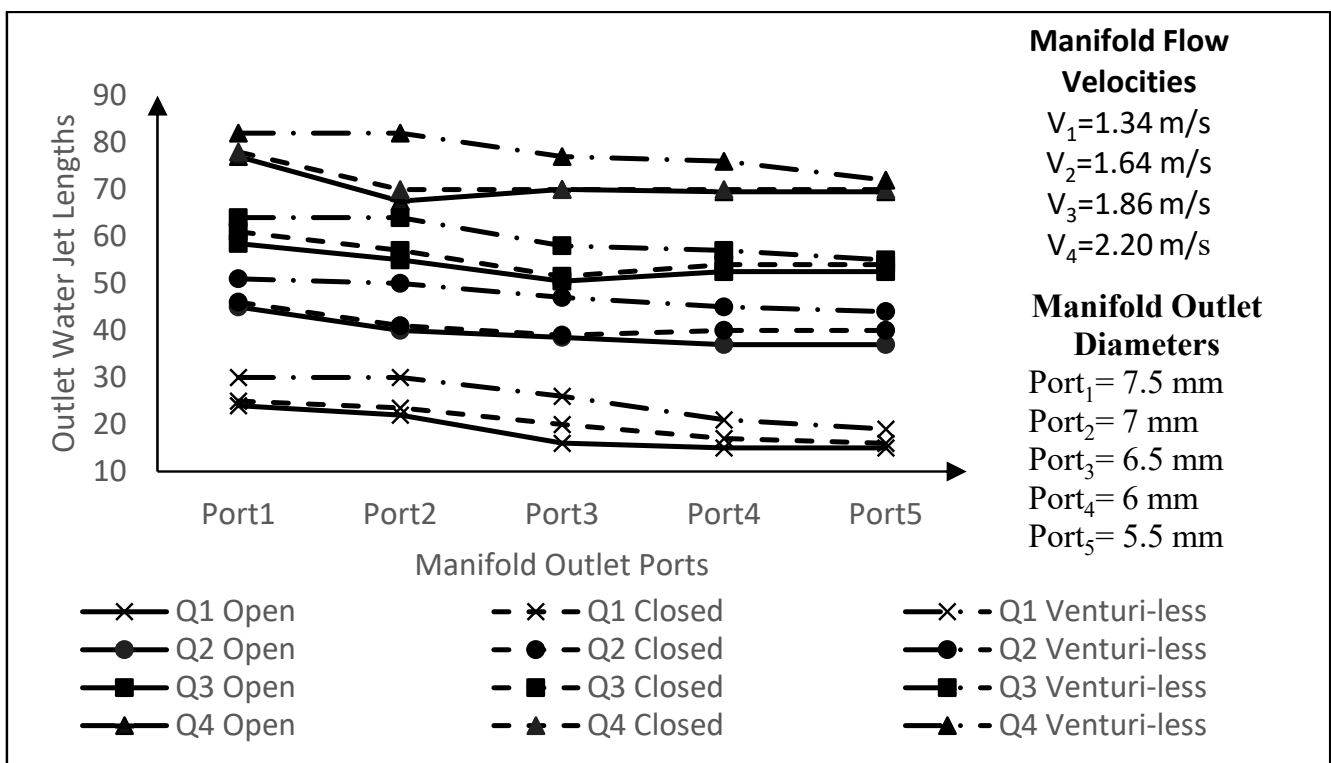
In this experiment set, when the jet nozzle exit diameters decreased and then remained constant while the flow rate increased, the jet lengths in the first two port exits were close in value, showed a significant drop at the third port exit, and were measured to be approximately the same as the jet lengths measured at the first two port exits at the fourth and fifth port exits. Additionally, it was measured that in the absence of a Venturi device, much larger jet lengths were obtained compared to the cases where the Venturi device was closed or open.

In the third experiment set, the aim was to compare the jet exit lengths obtained while using Venturi Type 1, Manifold Type 3, and the system without Venturi. The jet exit lengths were obtained for each nozzle with exit diameters of $d_1 = 7.5$ mm, $d_2 = 7$ mm, $d_3 = 6.5$ mm, $d_4 = 6$ mm, and $d_5 = 5.5$ mm and corresponding velocities of $V_1 = 1.34$ m/s, $V_2 = 1.64$ m/s, $V_3 = 1.86$ m/s, and $V_4 = 2.20$ m/s for both the Venturi and non-Venturi systems. The results are shown in Figure 9.
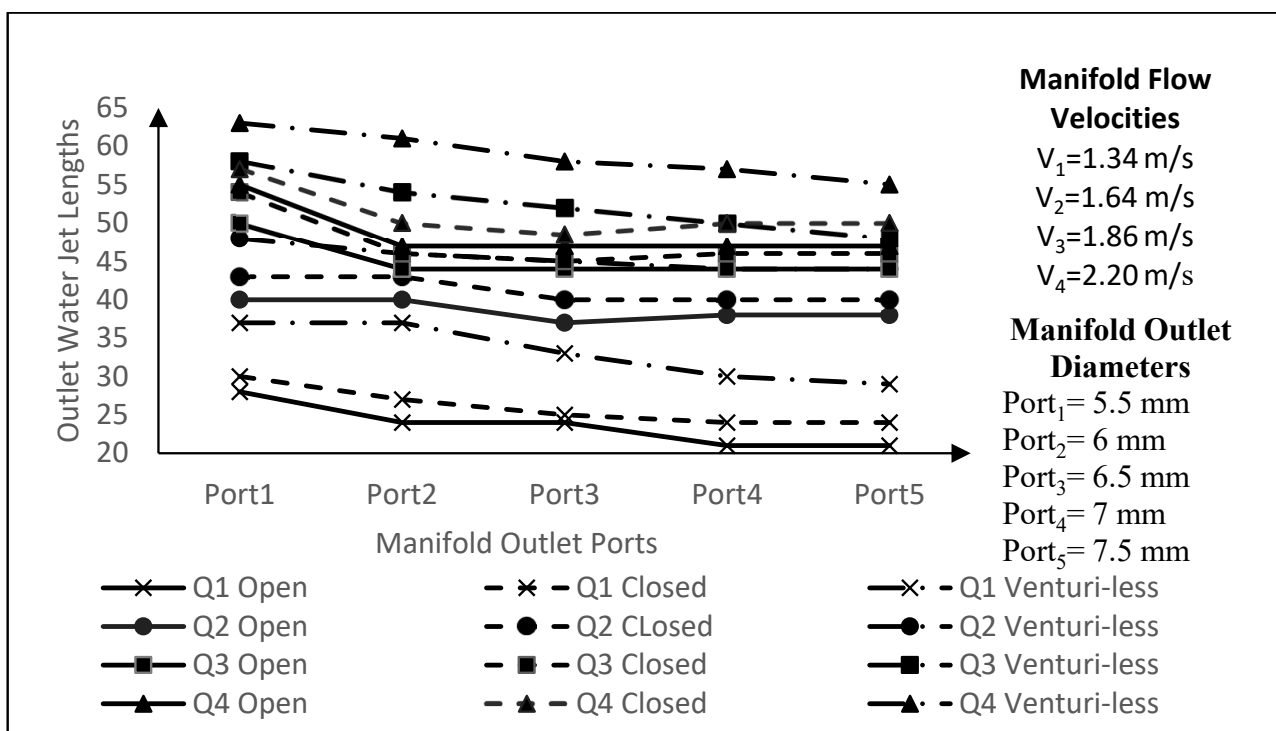
Figure 8. Graph of comparison of water jet lengths in Venturi Type 1 Manifold Type 2 open, closed, and Venturi deviceless systems ($Q_1 = 17 \times 10^{-5}$ m^3/s, $Q_2 = 20.8 \times 10^{-5}$ m^3/s, $Q_3 = 23.6 \times 10^{-5}$ m^3/s, $Q_4 = 27.8 \times 10^{-5}$ m^3/s).

Figure 9. Graph of comparison of water jet lengths in Venturi Type 1 Manifold Type 3 open, closed and Venturi deviceless systems ($Q_1 = 17 \times 10^{-5}$ m^3/s, $Q_2 = 20.8 \times 10^{-5}$ m^3/s, $Q_3 = 23.6 \times 10^{-5}$ m^3/s, $Q_4 = 27.8 \times 10^{-5}$ m^3/s).

In this experiment set, it was observed that when the jet nozzle exit diameters decreased, the jet exit lengths also decreased depending on the changes in diameter, provided that the flow rate was constant. Similarly, in this experiment set, it was observed that the jet exit lengths increased when the flow rate increased, provided that the jet nozzle exit diameters remained constant. Additionally, in the absence of a Venturi device, the observed jet length variations were not as pronounced as in the cases where the Venturi device was closed or open. It was also observed that the significant increase in jet lengths in the non-Venturi system occurred in this experiment set as well.

In the fourth experiment set, the aim was to compare the jet exit lengths obtained while using Venturi Type 1, Manifold Type 4, and the system without Venturi. The jet exit lengths were obtained for each nozzle with exit diameters of d_1 = 5.5 mm, d_2 = 6 mm, d_3 = 6.5 mm, d_4 = 7 mm, and d_5 = 7.5 mm and corresponding velocities of V_1 = 1.34 m/s, V_2 = 1.64 m/s, V_3 = 1.86 m/s, and V_4 = 2.20 m/s for both the Venturi and non-Venturi systems. The results are shown in Figure 10.
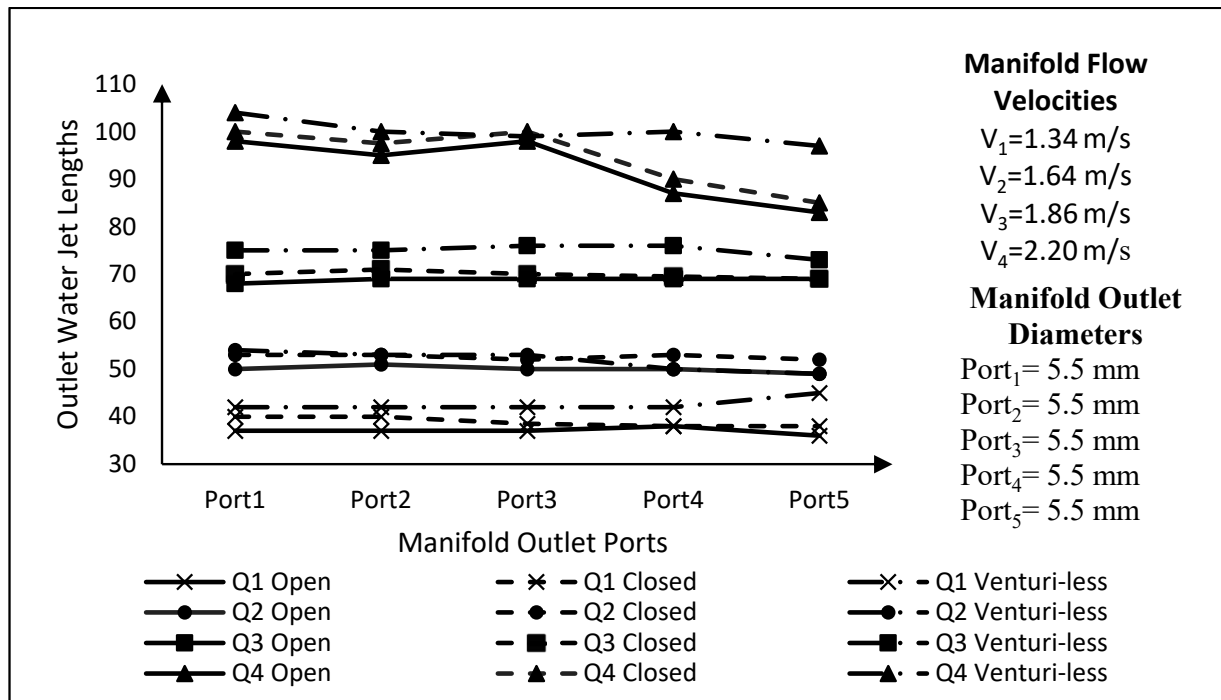

Figure 10. Graph of comparison of water jet lengths in Venturi Type 1 Manifold Type 4 open, closed, and Venturi deviceless systems ($Q_1 = 17 \times 10^{-5}$ m^3/s, $Q_2 = 20.8 \times 10^{-5}$ m^3/s, $Q_3 = 23.6 \times 10^{-5}$ m^3/s, $Q_4 = 27.8 \times 10^{-5}$ m^3/s).

In this experiment set, it was observed that when the jet nozzle exit diameters increased, the jet exit lengths decreased depending on the changes in diameter, provided that the flow rate was constant. Similarly, in this experiment set, it was observed that the jet exit lengths increased when the flow rate increased, provided that the jet nozzle exit diameters remained constant. Additionally, it was observed that in the absence of a Venturi device, larger jet lengths were formed compared to the cases where the Venturi device was closed or open.

2.3.2. Comparison of Jet Exit Length Measurements in Open and Closed Venturi Type 2 Systems and Systems Without Venturi

In the first experiment set, the aim was to compare the jet exit lengths obtained while using Venturi Type 2, Manifold Type 1, and the system without Venturi. The jet exit lengths were obtained for each nozzle with exit diameters of d_1 = 5.5 mm, d_2 = 5.5 mm, d_3 = 5.5 mm,

d_4 = 5.5 mm, and d_5 = 5.5 mm and corresponding velocities of V_1 = 1.34 m/s, V_2 = 1.64 m/s, V_3 = 1.86 m/s, and V_4 = 2.20 m/s for both the Venturi and non-Venturi systems. The results are shown in Figure 11.

Figure 11. Graph of comparison of water jet lengths in Venturi Type 2 Manifold Type 1 open, closed, and Venturi deviceless systems (Q_1 = 17 × 10^{-5} m^3/s, Q_2 = 20.8 × 10^{-5} m^3/s, Q_3 = 23.6 × 10^{-5} m^3/s, Q_4 = 27.8 × 10^{-5} m^3/s).

From this experiment set, it was observed that there was no change in jet exit lengths with constant jet nozzle exit diameter and flow rate. It was also observed that the jet exit lengths increased with increasing flow rates while the jet nozzle exit diameter remained constant. Furthermore, it was observed that much larger jet lengths were formed in the absence of a Venturi device compared to the cases where the Venturi device was closed or open. As a result, homogeneous jet lengths were obtained at low main manifold flows and equal exit port nozzle diameters.

In the second experiment set, the aim was to compare the jet exit lengths obtained while using Venturi Type 2, Manifold Type 2, and the system without Venturi. The jet exit lengths were obtained for each nozzle with exit diameters of d_1 = 6.5 mm, d_2 = 6 mm, d_3 = 5.5 mm, d_4 = 5.5 mm, and d_5 = 5.5 mm and corresponding velocities of V_1 = 1.34 m/s, V_2 = 1.64 m/s, V_3 = 1.86 m/s, and V_4 = 2.20 m/s for both the Venturi and non-Venturi systems. The results are shown in Figure 12.
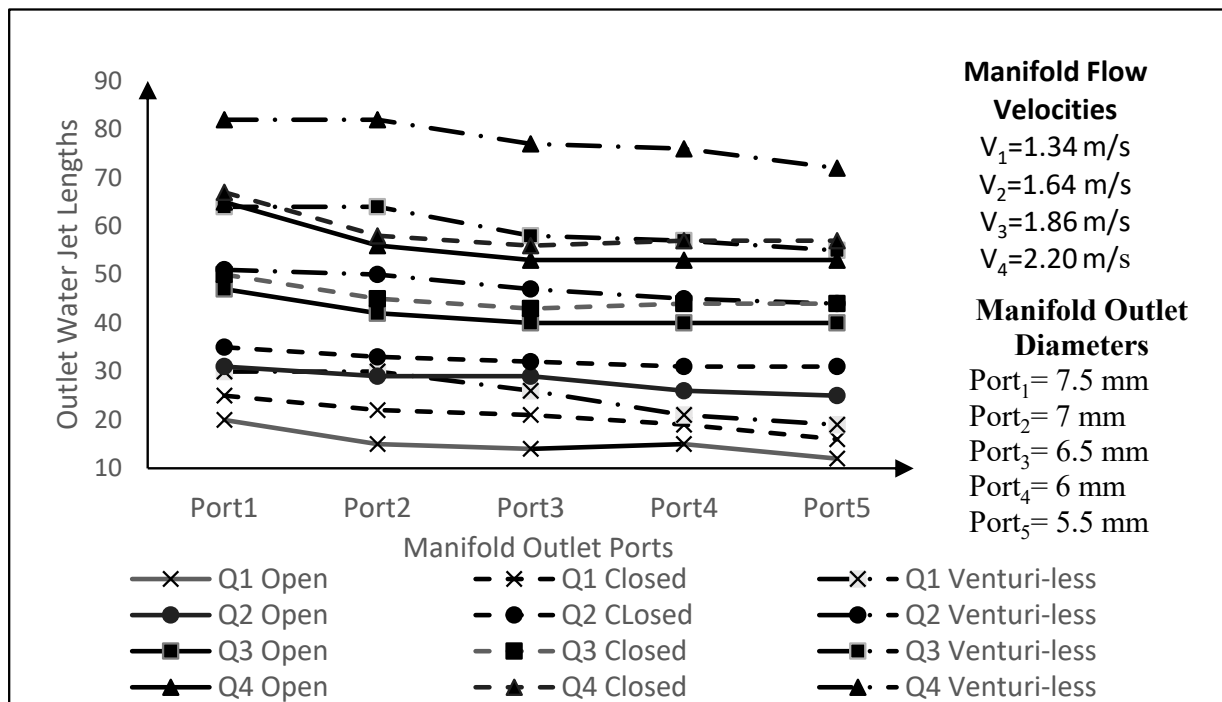
In this experiment set, it was observed that when the jet nozzle exit diameters decreased and then stabilized, and the flow rate increased, the jet lengths of the first two port exits were close to each other, and there was a significant decrease at the third port exit, and the jet lengths measured at the fourth and fifth port exits were close to the lengths measured at the first two port exits. Additionally, it was measured that much larger jet lengths were obtained in the absence of a Venturi device compared to the cases where the Venturi device was closed or open.

In the third experiment set, the aim was to compare the jet exit lengths obtained while using Venturi Type 2, Manifold Type 3, and the system without Venturi. The jet exit lengths were obtained for each nozzle with exit diameters of d_1 = 7.5 mm, d_2 = 7 mm, d_3 = 6.5 mm, d_4 = 6 mm, and d_5 = 5.5 mm and corresponding velocities of V_1 = 1.34 m/s, V_2 = 1.64 m/s,

V_3 = 1.86 m/s, and V_4 = 2.20 m/s for both the Venturi and non-Venturi systems. The results are shown in Figure 13.
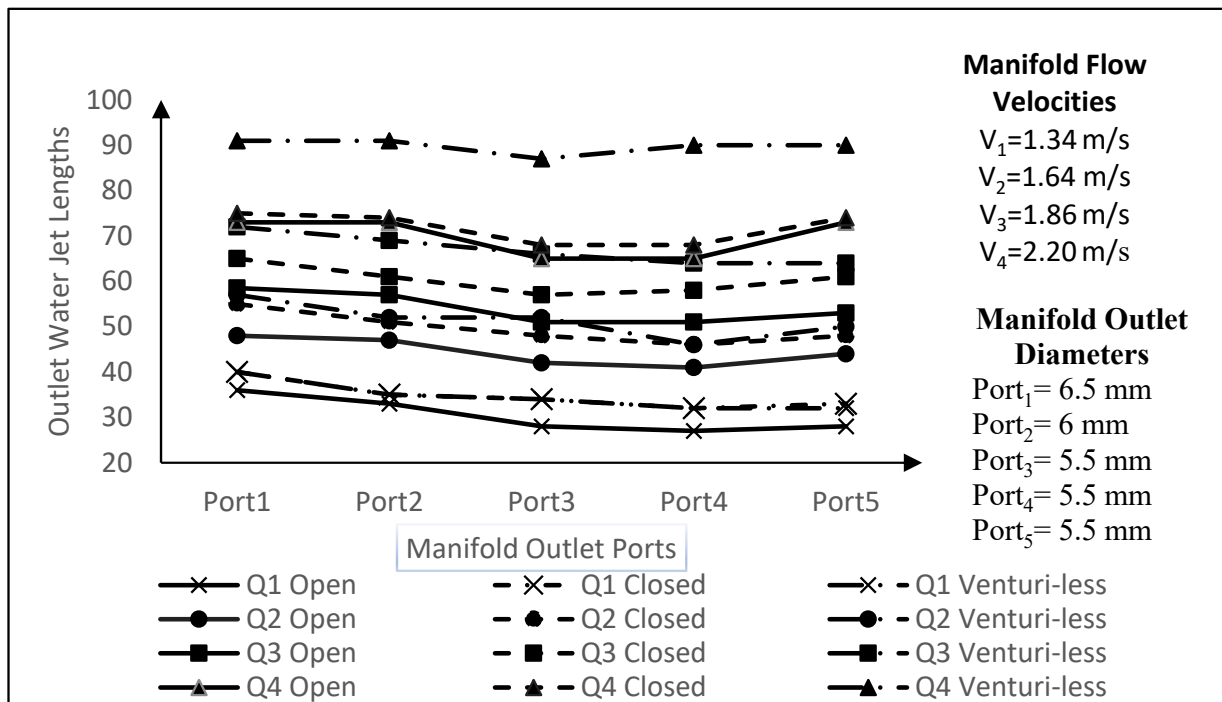
Figure 12. Graph of comparison of water jet lengths in Venturi Type 2 Manifold Type 2 open, closed, and Venturi deviceless systems ($Q_1 = 17 \times 10^{-5}$ m^3/s, $Q_2 = 20.8 \times 10^{-5}$ m^3/s, $Q_3 = 23.6 \times 10^{-5}$ m^3/s, $Q_4 = 27.8 \times 10^{-5}$ m^3/s).

Figure 13. Graph of comparison of water jet lengths in Venturi Type 2 Manifold Type 3 open, closed and Venturi deviceless systems ($Q_1 = 17 \times 10^{-5}$ m^3/s, $Q_2 = 20.8 \times 10^{-5}$ m^3/s, $Q_3 = 23.6 \times 10^{-5}$ m^3/s, $Q_4 = 27.8 \times 10^{-5}$ m^3/s).

In this experiment set, it was observed that the jet exit lengths decreased depending on the changes in diameter when the jet nozzle exit diameters decreased while the flow rate remained constant. It was also observed that the jet exit lengths increased when the flow rate increased while the jet nozzle exit diameters remained constant. Furthermore, it was observed that the pronounced breaks seen in the cases where the Venturi device was closed or open were not present in the absence of a Venturi device. The distinct increase observed in the non-Venturi system was also observed in this experiment set.

In the fourth experiment set, the aim was to compare the jet exit lengths obtained while using Venturi Type 2, Manifold Type 4, and the system without Venturi. The jet exit lengths were obtained for each nozzle with exit diameters of d_1 = 5.5 mm, d_2 = 6 mm, d_3 = 6.5 mm, d_4 = 7 mm, and d_5 = 7.5 mm and corresponding velocities of V_1 = 1.34 m/s, V_2 = 1.64 m/s, V_3 = 1.86 m/s, and V_4 = 2.20 m/s for both the Venturi and non-Venturi systems. The results are shown in Figure 14.
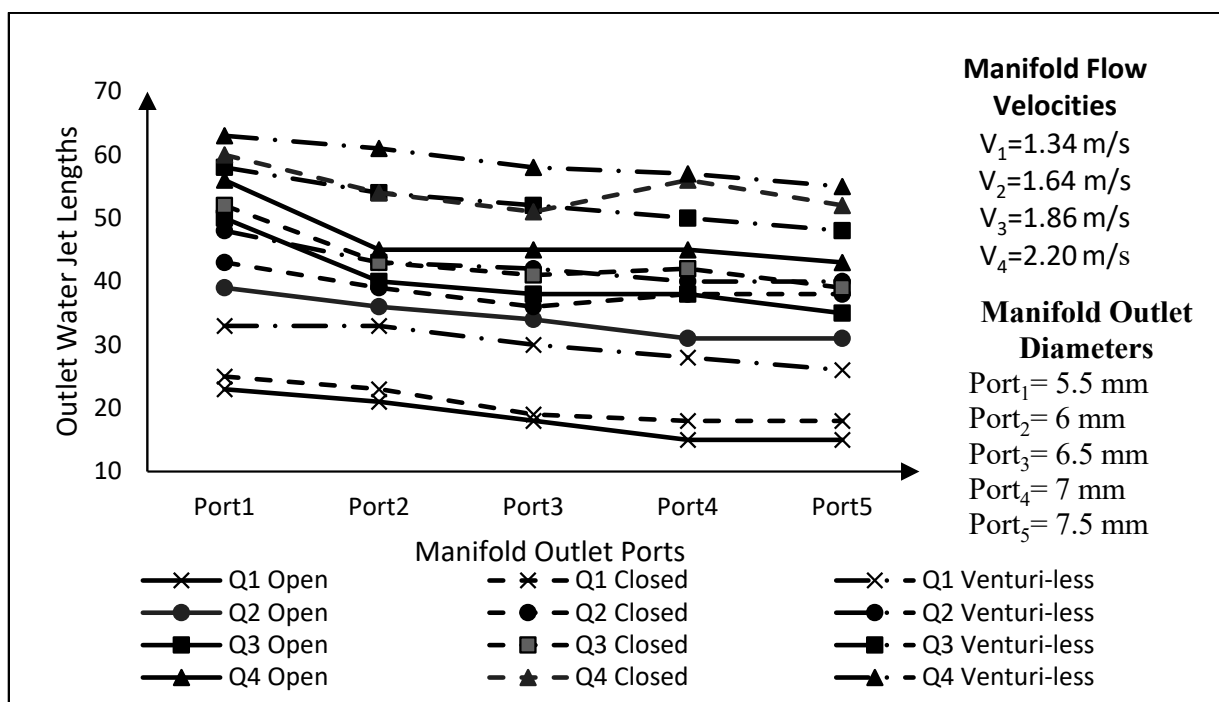

Figure 14. Graph of comparison of water jet lengths in Venturi Type 2 Manifold Type 4 open, closed, and Venturi deviceless systems ($Q_1 = 17 \times 10^{-5}$ m^3/s, $Q_2 = 20.8 \times 10^{-5}$ m^3/s, $Q_3 = 23.6 \times 10^{-5}$ m^3/s, $Q_4 = 27.8 \times 10^{-5}$ m^3/s).

In this experiment set, it was observed that the jet exit lengths decreased depending on the changes in diameter when the jet nozzle exit diameters increased while the flow rate remained constant. It was also observed that the jet exit lengths increased when the flow rate increased while the jet nozzle exit diameters remained constant. Furthermore, it was observed that larger jet lengths were formed in the absence of a Venturi device compared to the cases where the Venturi device was closed or open.

2.4. Dimensionless Parameter Analysis

A dimensionless parameter analysis was performed on the acquired experimental data. The parameters Q_s/Q_a and d_{port}/L_{jet} were investigated as the most suitable candidates. Consequently, the correlation coefficient R² for the equation developed for Venturi Type 1 was determined to be 0.541 (Figure 15). Measurement errors, calibration issues, and particularly jet characteristics (port exit diameter, jet breakup, jet fragmentation, and droplet formation) are believed to influence the experimental results. Moreover, the correlation coefficient R² for the equation developed for Venturi Type 2 was calculated as 0.689 (Figure 16).
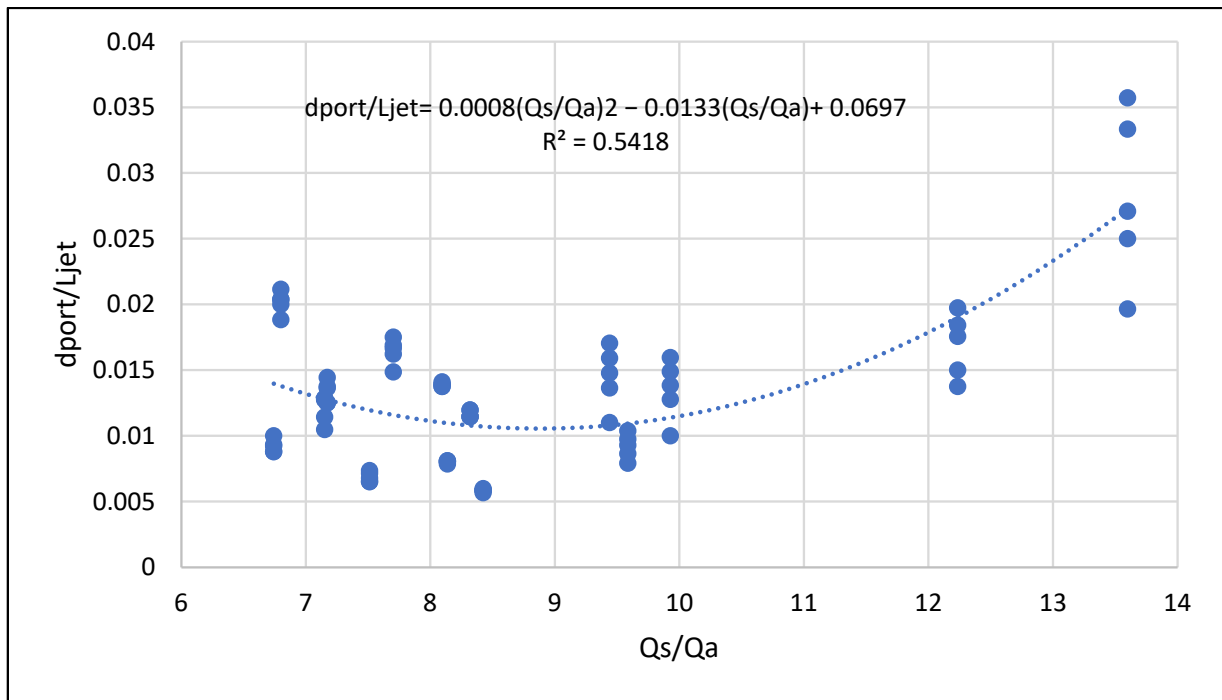
Figure 15. $D_{port}/L_{jet} - Q_s/Q_a$ scattering diagram in Venturi Type 1 experiment set.
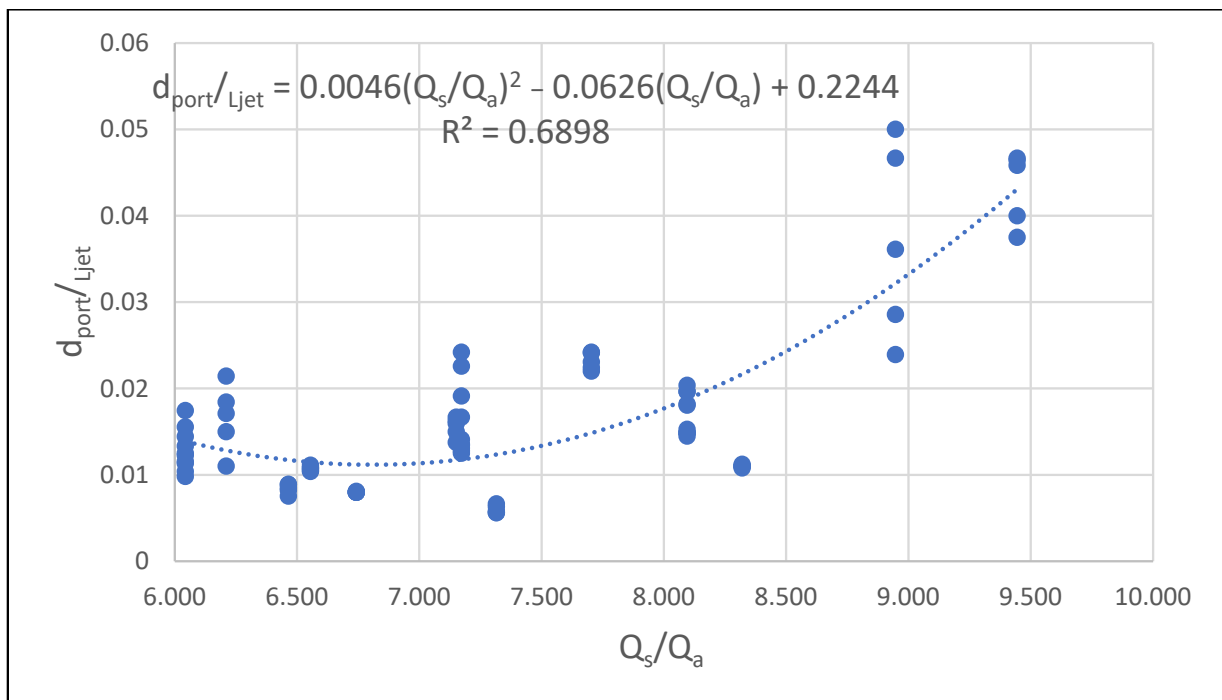

Figure 16. $D_{port}/L_{jet} - Q_s/Q_a$ scattering diagram in Venturi Type 2 experiment set.

2.5. Variation of Reynolds Number

The Reynolds number is a dimensionless parameter. It comes from analyzing the Navier–Stokes equations [21]. It provides information about whether a fluid flow is laminar or turbulent. The Reynolds number is calculated using the following equation:

$$Re = VD/\nu \qquad (1)$$

where Re is the Reynolds number, V is the manifold flow velocity (m/s), D is the manifold main pipe diameter (m), and ν is the kinematic viscosity of water (m^2/s).

The variation of the Reynolds number for the experimental system is summarized in Table 3: Change of Reynolds number.

Table 3. Change of Reynolds number.

Manifold Flow Velocity, m/s	Reynolds Number (Re)
V_1 = 1.34	16,850
V_2 = 1.64	20,620
V_3 = 1.86	23,388
V_4 = 2.20	27,663
D = 1.27×10^{-2} m, $\nu = 1.01 \times 10^{-6}$ m^2/s (for water temperature of 20 °C)	

3. Results and Discussion

Experimental measurements were conducted on the experimental setups, and the schematic diagrams are presented in Figures 2 and 3. The experimental measurements primarily consisted of water flow rate and water jet length. The results obtained from these measurements are graphically expressed.

Furthermore, the effects of differently designed experimental setups on the water and air–water (two-phase) mixture flow models, as well as the changes in the outlet flow values and behaviors, were experimentally investigated for different port exit diameters. The impact of different air–water flow rates on the outlet flows and manifold port exit diameters were compared using measurements of the outlet jet lengths. The experimental results obtained were conducted with different manifold types and Venturi devices and presented graphically, thus enabling data interpretation. Additionally, dimensionless parameter analyses and numerical modeling studies were performed. With the data obtained from the experiments tested with different flow rates using the Venturi Type 1 device, a dimensionless equation was created as $d_{port}/L_{jet} = 0.0008(Q_s/Q_a)^2 - 0.0133(Q_s/Q_a) + 0.0697$. With the data obtained from the experiments tested with different flow rates using the Venturi Type 2 device, a dimensionless equation was created as $d_{port}/L_{jet} = 0.0046(Q_s/Q_a)^2 - 0.0626(Q_s/Q_a) + 0.2244$. The dimensionless parameters obtained and the numerical modeling studies allow for the prediction of results for untested conditions.

During the experimental studies, it was observed that the water jets exiting from the manifold ports fragmented and subsequently formed droplets. It was determined that such formations occur, especially in two-phase flows. The cause of jet breakup and droplet formation is thought to be related to jet stability, two-phase characteristics, port exit diameters, and velocities. The significant results obtained from these findings are listed in the following section.

In the experimental studies, the water jet lengths corresponding to each flow rate in different manifold types at low flow rates were measured as homogeneous (close to each other in length) (Figures 11–14).

Analyses can be conducted with experimental setups of different sizes (increased main manifold pipe diameter and port outlet diameter) and at various flow rates (increased velocities). The experimental setup can be integrated into water-immersed systems for further studies. Hydraulic erosion characteristics can be investigated in an integrated system filled with a newly designed fine sand reservoir.

4. Conclusions

The two-phase system (equipped with a Venturi device) was initially operated at various d/D ratios, with values recorded below 0.4. The first critical value of this ratio was determined to be d/D = 0.433. At this critical value, a water flow was observed in the system.

The results obtained from the experimental study indicate that uniform jet exit lengths are achieved at low flow rates. When the main manifold flow velocity *V* was between 1.5 and 2 m/s, the system exhibited stable operation and produced high jet lengths. Additionally, it provided suitable operating conditions for d/D = 0.433. The system did not meet two-phase flow conditions at ratios below this critical value. The system does not show a smooth flow pattern with Venturi devices for d/D < 0.433. The low flow rates used in this study's experimental sets are considered an important parameter for the design of micro irrigation systems depending on the critical d/D ratio of the system.

As expected, a flow velocity of around $1-2$ m/s, which is considered ideal for low head losses in hydraulic systems, was also observed in this study.

The fundamental parameters identified for the system were d, D, Lj, Q_s, and Q_a.

Based on the main manifold flow velocities of V_1 = 1.34 m/s, V_2 = 1.64 m/s, V_3 = 1.86 m/s, and V_4 = 2.20 m/s in this study, Reynolds numbers of 16,850, 20,620, 23,388, and 27,663 were obtained, respectively.

In the study, the air suction flow rate measured in both Venturi devices increases with increasing flow rate. It was also observed that the water jet lengths increase in a similar way.

During the experimental studies, it was observed that the water jets discharged from the manifold ports fragmented and subsequently formed droplets. These formations were particularly observed in two-phase flows.

The parameters Q_s/Q_a and d_{port}/L_{jet} were investigated as the most suitable candidates. Accordingly, the correlation coefficient R^2 of the equation developed for Venturi Type 1 was calculated as 0.541. Additionally, the correlation coefficient R^2 of the equation developed for Venturi Type 2 was calculated as 0.689. It is thought that the factors affecting the results of the experimental study are measurement errors, calibration problems, and especially jet characteristics (port exit diameter, jet breakup, jet fragmentation, and droplet formation).

Author Contributions: Methodology: S.T. and T.B. Validation: T.B. and S.T. Formal Analysis: S.T., A.A., and T.B. Investigation: S.T. Data curation: S.T. and A.A. Writing—Original Draft Preparation: S.T. and A.A. Writing review and editing: S.T., A.A., and T.B. Visualization: S.T. and A.A. Supervision: T.B. and S.T. Project Administration: T.B. and S.T. Funding Acquisition: S.T. All authors have read and agreed to the published version of the manuscript.

Conflicts of Interest: The authors declare no conflict of interest.

References

1. Mareels, I.; Weyer, E.; Ooi, S.K.; Cantoni, M.; Li, Y.; Nair, G. Systems Engineering for irrigation systems: Successes and Challenges. In Proceedings of the 16th Triennial World Congress, Prague, Czech Republic, 4–8 July 2005.
2. Bagatur, T.; Onen, F. A Predictive Model on Air Entrainment by Plunging Water Jets using GEP and ANN. *KSCE J. Civ. Eng.* **2014**, *18*, 304–314. [CrossRef]
3. Bagatur, T. *Su jeti ile Havalandırma Sistemlerinde Ağızlık Tipinin Havalandırma Performansına Etkisi*; Fırat University Institute of Science: Elazığ, Türkiye, 2000.
4. Baylar, A.; Emiroglu, M.E. Air Entrainment and Oxygen Transfer in a Venturi. In *Proceedings of the Institution of Civil Engineers—Water and Maritime Engineering*; Thomas Telford Ltd.: London, UK, 2003; pp. 249–255.
5. Öztürkmen, G. *Membran Biyoreaktörlerde Venturi Enjektörü Kullanilarak Işletme Şartlarinin Iyileştirilmesinin Araştirilmasi*; Dicle University Institute of Science: Diyarbakır, Türkiye, 2018.
6. Carrión, P.; Tarjuelo, J.; Montero, J. SIRIAS: A simulation model for sprinkler irrigation. *Irrig. Sci.* **2001**, *20*, 73–84. [CrossRef]
7. Issaka, Z.; Li, H.; Tang, P.; Yue, J.; Darko, R.O. Water-smart sprinkler irrigation, prerequisite to climate change adaptation: A review. *J. Water Clim. Chang.* **2018**, *9*, 383–398. [CrossRef]
8. Kaur, P.; Kaur, K.; Singh, H. Role of Micro-Irrigation in Vegetable Crops. *Int. J. Agric. Innov. Res.* **2020**, *9*, 89–96.
9. Subaschandar, N.; Sakthivel, G. Performance Improvement of a Typical Manifold using Computational Fluid Dynamics. In *MATEC Web of Conferences*; EDP Sciences: Paris, France, 2016.

10. Hassan, J.M.; Mohamed, T.A.; Mohammed, W.S.; Alawee, W.H. Modeling the Uniformity of Manifold with Various Configurations. *J. Fluids* **2014**, *2014*, 325259. [CrossRef]
11. Alawee, W.H.; Hassan, J.M.; Mohammad, W.S. Effect of variation of the diameter of the inlet to the distribution manifold on flow uniformity in dividing manifold system. *Quest J. J. Res. Appl. Math.* **2021**, *7*, 9–13.
12. Jiang, Y.; Alawee, W.H.; Essa, F.A.; Abdullah, A.S.; Omara, Z.M.; Ahmad, H.; Ali, R.; Wang, F.; Menni, Y. Effect of area ratio and Reynolds number on the distribution of discharge in dividing manifold. *Int. J. Low Carbon Technol.* **2022**, *17*, 1271–1279. [CrossRef]
13. Han, S.-S.; Bae, T.-H.; Jang, G.-G.; Tak, T.-M. Influence of sludge retention time on membrane fouling and bioactivities in membrane bioreactor system. *Process Biochem.* **2005**, *40*, 2393–2400. [CrossRef]
14. Brijesh, R.N.; Sagar, M.P. The Effect of Venturi Design on Jet Pump Performance. *J. Res.* **2016**, *2*, 23–28.
15. Mayer, M.; Braun, R.; Fuchs, W. Comparison of various aeration devices for air sparging in crossflow membrane filtration. *J. Membr. Sci.* **2006**, *277*, 258–269. [CrossRef]
16. Çakir, A.; Çaliş, H. *Uzaktan Kontrollü Otomatik Sulama Sistemi Tasarımı ve Uygulaması*; Süleyman Demirel Üniversitesi Fen Bilimleri Enstitüsü Dergisi: Isparta, Turkey, 2007.
17. Sudharshan, N.; Karthik, A.K.; Kiran, J.S.; Geetha, S. Renewable Energy Based Smart Irrigation System. *Procedia Comput. Sci.* **2019**, *165*, 615–623. [CrossRef]
18. Steven, R. A dimensional analysis of two phase flow through a horizontally installed Venturi flow meter. *Flow Meas. Instrum.* **2008**, *19*, 342–349. [CrossRef]
19. Ma, J.; Zhu, D.Z.; Rajaratnam, N.; Camino, G.A. Experimental Study of the Breakup of a Free-Falling Turbulent Water Jet in Air. *J. Hydraul. Eng.* **2016**, *142*, 06016014. [CrossRef]
20. Kenneth Balkey, P.E.; Canonico, D.A.; Guzman, A.L.; Nelson, P.F.; Mark Webster, P.E.; Weinman, S. *Examples of Use of Codes and Standards for Students in Mechanical Engineering and Other Fields*; ASME: New York, NY, USA, 2021.
21. Kirkgoz, M.S. *Akışkanlar Mekaniği*; Birsen Yayınevi: İstanbul, Türkiye, 2013.